BBA - Molecular Cell Research 1868 (2021) 118989

Contents lists available at ScienceDirect

BBA - Molecular Cell Research

journal homepage: www.elsevier.com/locate/bbamcr

Characterization of mitochondrial calpain-5

Yusaku Chukai [a], Takeshi Iwamoto [a], Ken Itoh [b], Hiroshi Tomita [c], Taku Ozaki [a,*]

[a] Laboratory of Cell Biochemistry, Department of Biological Science, Graduate School of Science and Engineering, Iwate University, 4-3-5 Ueda, Morioka, Iwate 020-8551, Japan
[b] Department of Stress Response Science, Center for Advanced Medical Research, Hirosaki University Graduate School of Medicine, 5 Zaifuchou, Hirosaki, Aomori 036-8562, Japan
[c] Laboratory of Visual Neuroscience, Department of Biological Science, Graduate School of Science and Engineering, Iwate University, 4-3-5 Ueda, Morioka, Iwate 020-8551, Japan

ARTICLE INFO

Keywords:
Mitochondria
Calpain-5
Autolysis
ER stress
Retina
Liver

ABSTRACT

Calpain, a Ca^{2+}-dependent cysteine protease, plays a significant role in gene expression, signal transduction, and apoptosis. Mutations in human calpain-5 cause autosomal dominant neovascular inflammatory vitreoretinopathy and the inhibition of calpain-5 activity may constitute an effective therapeutic strategy for this condition. Although calpain-5 is ubiquitously expressed in mammalian tissues and was recently found to be present in the mitochondria as well as in the cytosol, its physiological function and enzymological properties require further elucidation. The objective of the current study was to determine the characteristics of mitochondrial calpain-5 in porcine retinas, human HeLa cells, and C57BL/6J mice using subcellular fractionation. We found that mitochondrial calpain-5 was proteolyzed/autolyzed at low Ca^{2+} concentrations in mitochondria isolated from porcine retinas and by thapsigargin-induced endoplasmic reticulum (ER) stress in HeLa cells. Further, mitochondrial calpain-5, as opposed to cytosolic calpain-5, was activated during the early stages of ER stress in C57BL/6J mice. These results showed that mitochondrial calpain-5 was activated at low Ca^{2+} concentrations *in vitro* and in response to ER stress *in vivo*. The present study provides new insights into a novel calpain system in the mitochondria that includes stress responses during the early phases of ER stress. Further, activation of mitochondrial calpain-5 by treatment using low-molecular-weight compounds may have therapeutic potential for diseases related to ER stress, including neurodegenerative diseases, metabolic syndromes, diabetes, and cancer.

1. Introduction

The Ca^{2+}-dependent cysteine protease calpain plays a significant role in gene expression, signal transduction, cell migration, and apoptosis [1–4]. Calpain-5 is one of 15 known calpain isoforms. Mutations of *CAPN5*, which encodes the human calpain-5, can cause autosomal dominant neovascular inflammatory vitreoretinopathy (ADNIV), a severe retinal disease [5] for which there are currently no available therapies. ADNIV is associated with mutations in the protease core domain of calpain-5 that result in hyperactivity, suggesting that inhibition of calpain-5 activity may constitute an effective therapeutic strategy for ADNIV [6]. Recently, Velez et al. reported the crystal structure of the calpain-5 protease core, enabling the guided design of inhibitors that specifically target mutated calpain-5 to treat ADNIV [7]. Notably, *CAPN5* null mice and photoreceptor-specific knockout mice do not show any abnormalities [6,8], further suggesting that the targeted inhibition of calpain-5 may be a viable therapy for ADNIV without adverse effects.

Some mitochondrial calpains, such as calpain-1 and calpain-2, have been well characterized both enzymologically and physiologically [9–11]. We have previously reported that mitochondrial calpain-1 and calpain-2 cooperatively regulate apoptosis-inducing factor (AIF)-dependent apoptotic cell death [9–11]. However, the functions of calpain-5, which is ubiquitously expressed in mammalian tissues [12]

Abbreviations: ADNIV, autosomal dominant neovascular inflammatory vitreoretinopathy; PDH, pyruvate dehydrogenase; DMEM, Dulbecco's Modified Eagle Medium; H_2O_2, hydrogen peroxide; ER, endoplasmic reticulum; DMSO, dimethyl sulfoxide; PEF, penta-EF.

* Corresponding author at: Laboratory of Cell Biochemistry, Department of Biological Science, Graduate School of Science and Engineering, Iwate University, 4-3-5 Ueda, Morioka, Iwate 020-8551, Japan.
E-mail address: tozaki@iwate-u.ac.jp (T. Ozaki).

https://doi.org/10.1016/j.bbamcr.2021.118989
Received 17 July 2020; Received in revised form 21 January 2021; Accepted 9 February 2021
Available online 16 February 2021

and is highly expressed in the central nervous system of rats [13], remains poorly understood. In particular, the enzymological properties and physiological functions of mitochondrial calpain-5 remain unclear. We recently reported that calpain-5 is localized in the mitochondria of porcine retinal photoreceptor cells [14], where the mitochondria are abundant [15], and that the molecular weight of intact mitochondrial calpain-5 (~70 kDa) is slightly lower than that of cytosolic calpain-5 (~75 kDa) [14]. We also found that two types of calpain-5, ~70 kDa and ~60 kDa forms, are present in the mitochondria of porcine retinas. Therefore, we sought to compare the molecular forms and enzymological properties of mitochondrial calpain-5 between several species and tissues.

In this study, we determined the autolysis of mitochondrial calpain-5, which reportedly parallels the activation of calpains and the dissociation of calpain subunits [16–18]; therefore, autolysis was evaluated as one of the enzymatic properties. Here, we sought to analyze the autolytic fragments of mitochondrial calpain-5 to examine its Ca^{2+}-sensitivity and response to ER stress. The purpose of this study was to determine and compare the enzymatic properties of cytosolic and mitochondrial calpain-5 in porcine retinas, human HeLa cells, and C57BL/6J mice to examine the characteristics of calpain-5 *in vitro* and *in vivo*.

2. Materials and methods

2.1. Subcellular fractionation

The subcellular fractionation was performed as previously described [13]. Briefly, porcine retinas and mouse livers were gently suspended in 2 volumes of mitochondrial isolation buffer (KC010100, BioChain Institute, Newark, CA, USA). The suspension was homogenized, following which the mitochondrial and cytosolic fractions were prepared *via* differential centrifugation. Mitochondrial fractions were washed thrice and resuspended in mitochondrial isolation buffer.

2.2. Proteinase K treatment of mitochondria

To examine whether calpain-5 exists in the mitochondria, the mitochondrial surface was treated with proteinase K as previously described [9]. Isolated mitochondria were suspended in mitochondrial isolation buffer (KC010100, BioChain Institute) and treated with proteinase K (P2308, Sigma-Aldrich, St. Louis, MO, USA) at a final concentration of 100 μg/ml for 30 min at 4 °C. Phenylmethylsulfonyl fluoride (PMSF, 10837091001, Sigma-Aldrich) was added to a final concentration of 2 mmol/L, and samples were incubated for a further 10 min at 4 °C before western blot and proteolysis/autolysis assays were performed.

2.3. In vitro calpain-5 proteolysis/autolysis assay

A proteolysis/autolysis assay was performed to first determine whether Ca^{2+} was required for calpain-5 activation *in vitro* and identify the minimum amount of Ca^{2+} required to activate calpain-5. Soluble mitochondrial fractions (intermembrane space and matrix) were prepared by sonicating the mitochondrial suspension and centrifugation at 100,000 ×*g* for 30 min. To evaluate the Ca^{2+}-sensitivity of mitochondrial and cytosolic calpain-5, the mitochondrial and cytosolic fractions were incubated with $CaCl_2$ at a final concentration of 1000 μM for 0–120 min. To identify the Ca^{2+} concentrations required to autolyze calpain-5, mitochondrial and cytosolic fractions were incubated with different concentrations of Ca^{2+} (final concentrations from 0 to 1000 μM) for 120 min. To examine whether proteolysis/autolysis of calpain-5 was inhibited by calpain inhibitors, calpeptin and PD150606 (final concentration of 10 μM and 5 μM, respectively) were pre-incubated for 1 h at 4 °C and then incubated with $CaCl_2$ at a final concentration of 1 mM for 120 min at 37 °C. All reactions were stopped by adding sample buffer solution (FUJIFILM Wako, Osaka, Japan) and boiling the mixtures at 90 °C for 3 min. Proteolytic/autolytic fragments of calpain-5 were detected by western blot.

2.4. Western blot analyses

Western blot analyses were performed as previously reported [13]. Briefly, following sodium dodecyl sulfate-polyacrylamide gel electrophoresis (SDS-PAGE) with 6%, 10%, 12.5%, 15% polyacrylamide gels and electrophoretic transfer to polyvinylidene difluoride (PVDF) membranes (pore size 0.45 μm, Immobilon-P membrane, IPVH00010, Millipore), the membranes were blocked using 1–5% skim milk or 0.5% bovine serum albumin and 1% goat serum in PBS-T (0.05% Tween 20, 0.14 M NaCl and 10 mM phosphate buffer, pH 7.4) for 1 h at room temperature. After blocking, the membranes were allowed to react with primary and secondary antibodies. Antibodies were diluted in PBS-T as follows: anti-calpain-5 (1:2000, GTX103264; GeneTex, Irvine, CA, USA), anti-beta-actin (1:5000, ab6276, Abcam, Cambridge, UK), anti-Tom20 (1:2000, sc-136211, Santa Cruz Biotechnology, Inc., Santa Cruz, CA, USA), anti-pyruvate dehydrogenase (PDH) subunit E1 alpha (1:2000, 459400, Invitrogen, Carlsbad, CA, USA), anti-Bip (1:5000, ab21685, Abcam), anti-ATF6α (1:500, sc-166659, Santa Cruz), anti-CHOP (1:500, sc-7351, Santa Cruz), anti-COX IV (1:5000, ab16056, Abcam), anti-GAPDH (1:1000, PA1-987, Invitrogen), anti-adenylate kinase 2 (AK2) (1:2000, PA5-49482, Invitrogen), anti-calnexin (1:500) [19], anti-LSD1 (1:500, sc-271720, Santa Cruz), anti-lamin A/C (1:500, sc-7293, Santa Cruz), horseradish peroxidase-conjugated polyclonal goat anti-rabbit (P0448) and rabbit anti-mouse (P0260) immunoglobulins (1:10,000, Dako, Carpinteria, CA, USA). The immunoreactive signals were developed with the ECL prime western blotting detection reagent (RPN2232, Cytiva, Tokyo, Japan). Images were captured using the C-DiGit blot scanner (M&S TechnoSystems, Osaka, Japan) and the ChemiDoc XRS Plus luminescent image analyzer (1708265J1PC, Bio-Rad, Hercules, CA, USA). Signal intensity was measured using the Image J software (NIH, Bethesda, MD, USA).

2.5. Cell culture

Human HeLa cells (No. RCB007) were obtained from RIKEN BioResource Research Center (RIKEN BRC). The cells were cultured in Dulbecco's modified Eagle's medium (DMEM; Nissui Pharmaceutical Co., Tokyo, Japan) together with 100 units/m of penicillin, 100 μg/ml streptomycin, 2 mM L-glutamine, and 10% fetal bovine serum. The cells were grown at 37 °C in an atmosphere containing 5% CO_2.

2.6. Immunocytochemistry in HeLa cells

HeLa cells (2×10^4 cells/well) were seeded on coverslips in a 96-well plate and incubated for 24 h at 37 °C under 5% CO_2 conditions. The cells were washed with PBS (0.14 M NaCl and 10 mM phosphate buffer, pH 7.4) and fixed with 4% paraformaldehyde in 0.1 M PBS for 15 min at 25 °C. The fixed cells were permeabilized with 0.2% Triton X-100 for 20 min at 25 °C, and subsequently incubated with 1% skim milk in PBS with added 0.05% Tween 20 (PBS-T) for 1 h at 25 °C. The cells were incubated overnight at 4 °C with rabbit polyclonal anti-calpain-5 (1:100, GTX103264, GeneTex) and mouse monoclonal anti-Tom20 antibodies (1:100, sc-136211, Santa Cruz Biotechnology) that were diluted in 1% skimmed milk in PBS-T. Cells were then incubated with goat anti-rabbit

IgG-Alexa Fluor 488 (1:200, A11034, Invitrogen) and goat anti-mouse IgG-Alexa Fluor Plus 594 (1:200, A11032, Invitrogen) diluted in 1% skimmed milk in PBS-T overnight at 4 °C. The stained slides were mounted using Vectashield H-1200 with DAPI (Vector Laboratories Inc., Burlingame, CA, USA). Immunofluorescent images were observed by fluorescence microscopy (DMi8, Leica, WZ, DEU).

2.7. Thapsigargin treatment in HeLa cells

To determine the association between ER stress and proteolysis/autolysis of calpain-5, HeLa cells (1.6×10^6 cells/100 mm dish) were treated with thapsigargin (FUJIFILM Wako, 205-17283). The chemical was dissolved in dimethyl sulfoxide (DMSO); the final concentration of DMSO in the DMEM was less than 0.1%. For western blot analysis, cells were suspended in mitochondrial isolation buffer (KC010100, BioChain Institute). The suspension was homogenized, following which the mitochondrial and cytosolic fractions were prepared *via* differential centrifugation. Mitochondrial fractions were washed twice and resuspended in mitochondrial isolation buffer. To obtain the whole cell lysates, the cells were homogenized with RIPA buffer (20 mM Tris-HCl, pH 7.4, 150 mM NaCl, 1 mM EDTA, 1% NP-40, 0.1% Sodium deoxycholate, 0.1% SDS). Then, we obtained the whole cell lysates by centrifugation at 20,000 ×*g* for 30 min. Each fraction was used for western blot analyses.

2.8. Knockdown of calpain-1, 2, 5, or GAPDH with specific siRNA in HeLa cells

To examine the physiological functions of calpain-5, small interfering RNAs (siRNAs) for *CAPN1*, *CAPN2*, *GAPDH*, and *CAPN5* were transfected into HeLa cells (3.5×10^3 cells/well). A final concentration of 25 nM each of siRNA was transfected into cells using Lipofectamine RNAi Max Transfection Reagent (13778100, Invitrogen). Opti-MEM I Reduced Serum Medium (Invitrogen) was used for transfections instead of DMEM medium. Western blot analyses were performed 72 h after transfection to confirm the knockdown of each protein. The viability of transfected cells was measured *via* MTS assay 96 h after transfection. The siRNA sequences used were: ON-TARGETplus Non-targeting Pool (siControl), 5′-UGGUUUACAUGUCGACUAA-3′, 5′-UGGUUUACAUGUUGUGUGA-3′, 5′-UGGUUUACAUGUUUUCUGA-3′, 5′-UGGUUUACAUGUUUUCCUA-3′ (D-001810-10-05, Dharmacon, CO, USA), hs.Ri.CAPN1.13.1 (siCAPN1), 5′-ACACUUGAAGCGUGACUUCUUCCTG-3′ (IDT, Coralville, IA, USA), hs.Ri.CAPN2.13.1 (siCAPN2), 5′-GUUGAUUCUACCAAACAACAGUCCA-3′ (IDT), hs.Ri.CAPN5.13.1 (siCAPN5), 5′-CGCCAAGAAGAUGUCACUUGUUUAC-3′ (IDT), hs.Ri.GAPDH.13.1 (siGAPDH), 5′-GCUCAUUUCCUGGUAUGACAACGAA-3′ (IDT). For western blot analyses and the MTS assay, 3.0×10^5 and 3.0×10^3 cells were seeded in a 60 mm dish and a 96-well plate, respectively, 24 h before transfection.

2.9. MTS assay in HeLa cells

MTS assays were performed to determine the cell viability of *CAPN1*, *CAPN2*, *CAPN5*, and *GAPDH* knockdown cells. First, 1×10^4 cells were seeded in a 96-well plate. After 24 h, 20 μl of CellTiter 96® AQueous One Solution Cell Proliferation Assay (Promega, Madison, WI, USA) was added to the medium, and the mixture was incubated at 37 °C for 1 h. Following incubation, the absorbance at 490 nm was measured using a microplate leader (Infinite 200 PRO, TECAN, Männedorf, SUI).

2.10. ATP measurement in HeLa cells

The IntraCellular ATP kit ver.2 (TOYO B-Net, Tokyo, Japan) was used to measure ATP concentrations in siRNA-transfected cells. The cells were washed with PBS 96 h after transfection. After washing, intracellular ATP was extracted using an ATP extraction reagent. Next, 10 μl of the extract was allowed to react with 100 μl of an ATP luminescence reagent and the intensity of luminescence was measured at 460 nm using a microplate reader (TECAN).

2.11. Tunicamycin treatment and subcellular fractionation in C57BL/6J mice

All animal experiments complied with the ARRIVE guidelines and were carried out as per the U.K. Animals (Scientific Procedures) Act, 1986, and the associated guidelines EU Directive 2010/63/EU for animal experiments. The mouse experiments were approved by the Committee for the Ethics of Animal Experimentation of Iwate University and were carried out according to the Guidelines for Animal Experimentation of Iwate University. Mice were maintained in temperature-controlled conditions on a 12 h light-dark cycle. Tunicamycin was diluted in 150 mM dextrose to obtain a 0.1 μg/μl tunicamycin solution and a vehicle consisting of 1% DMSO in 150 mM dextrose was prepared. Eight-week-old C57BL/6J male mice were intraperitoneally injected with tunicamycin at 1 μg/g body mass. Mice were sacrificed 24 h after injection *via* cervical dislocation and their livers were enucleated. The enucleated livers were observed for pathology using a stereomicroscope (S9D, Leica). To obtain mitochondrial and cytosolic fractions, the livers were homogenized with mitochondrial isolation buffer (KC010100, BioChain Institute). Next, mitochondrial and cytosolic fractions were prepared *via* differential centrifugation. Then, calpain-5, cleaved ATF6, and cytochrome *c* were detected using western blot. To obtain the whole cell lysates, the livers were homogenized with RIPA buffer (20 mM Tris-HCl, pH 7.4, 150 mM NaCl, 1 mM EDTA, 1% NP-40, 0.1% Sodium deoxycholate, 0.1% SDS). Then, whole cell lysates were obtained by centrifugation at 20,000 ×*g* for 30 min, and the expression of ATF6, CHOP and Bip was detected using western blot.

2.12. Measurement of the mitochondrial outer membrane integrity

We measured the mitochondrial outer membrane integrity using a mitochondrial isolation kit (KC010100, BioChain Institute) and a mitochondrial activity assay kit (KC310100, BioChain Institute). Isolated mitochondria were resuspended in mitochondrial storage buffer. We diluted two samples in parallel of the mitochondrial suspension to 0.2 mg protein/m with either 1× enzyme dilution buffer (to measure cytochrome *c* oxidase activity in intact mitochondria) or using enzyme dilution buffer containing 1× n-Dodecyl β-D-maltoside (to measure the total cytochrome *c* oxidase activity). The diluted samples were incubated on ice for 15 min. Next, 2 μg of mitochondrial protein was measured for cytochrome *c* oxidase activity, and as per the manufacturer's instructions, the activity and the degree of mitochondrial integrity of each sample was calculated.

2.13. Statistical analysis

The Mann-Whitney *U* test was used for the MTS (Fig. 4e), ATP (Fig. 4f), and mitochondrial activity assays (Fig. 6i). *P* values were adjusted for multiple comparisons using the Bonferroni correction. A *P* value < 0.05 was used to indicate statistical significance. All data were analyzed using the Statistical Package for the Social Sciences (SPSS) 26.0 (IBM Corp., Armonk, NY, USA).

STAR★METHODS

KEY RESOURCES TABLE

REAGENT or RESOURCE	SOURCE	IDENTIFIER
Antibodies		
Calpain-5	GeneTex	GTX103264
Tom20	Santa Cruz	sc-136211
Pyruvate dehydrogenase	Invitrogen	459400
Adenylate Kinase 2 (AK2)	Invitrogen	PA5-49482
COXIV	Abcam	Ab16056
GAPDH	Invitrogen	PA1-987
beta-actin	Abcam	ab6276
Bip	Abcam	ab21685
ATF6	Santa Cruz	sc-166659
CHOP	Santa Cruz	sc-7351
LSD1	Santa Cruz	sc-271720
Lamin A/C	Santa Cruz	sc-7293
Chemicals		
mitochondrial isolation buffer	BioChain Institute	KC010100
proteinase K	Sigma-Aldrich	P2308
PMSF	Sigma-Aldrich	10837091001
Thapsigargin	FUJIFILM Wako	205-17283
Tunicamycin	Cayman Chemical	11445
Lipofectamine RNAi Max	Invitrogen	13778100
Experimental Models: Cell Line		
HeLa cell (Human)	RIKEN	RCB007
Experimental Models: Animal		
C57BL/6J mice	Japan SLC	C57BL/6JJmsSlc

3. Results

3.1. Enzymatic properties of cytosolic and mitochondrial calpain-5 in porcine retinas

To confirm the purity of cytosolic and mitochondrial fractions, we performed western blot analyses using following organelle marker: GAPDH for cytosol, AK2 for mitochondria, Calnexin for endoplasmic reticulum, and LSD1 for nucleus. We observed little cross contamination between each fraction and confirmed the high purity of our fractionations (Fig. 1a). Calpain-5 was detected in the mitochondrial fraction following Proteinase K treatment, which has been widely used to selectively remove proteins from the outer surface of mitochondrial outer membranes (Fig. 1b). Our results showed that proteinase K treatment did not remove mitochondrial calpain-5, and this was consistent with our previous report demonstrating that calpain-5 was present in all mitochondrial compartments [13]. Western blot analyses using antibodies that recognized the center region of calpain-5 showed that calpain-5 in the mitochondria had a slightly lower molecular weight than cytosolic calpain-5 (Fig. 1c). The molecular weights of the intact forms of cytosolic and mitochondrial calpain-5 were ~75 kDa and ~70 kDa, respectively. Additionally, cytosolic and mitochondrial calpain-5 produced proteolytic/autolytic fragments of ~37 kDa and ~30 kDa, respectively, in the presence of Ca^{2+}. The proteolysis/autolysis of calpain-5 was inhibited by the pan-calpain inhibitor calpeptin but not by PD150606, a selective inhibitor of calpains 1 and 2 (Fig. 1d and e), regardless of localization.

Proteolysis/autolysis assays were performed to examine the Ca^{2+}sensitivity of cytosolic and mitochondrial calpain-5 (Fig. 2). The ~37 kDa and ~30 kDa proteolytic/autolytic fragments were detected in the cytosol and mitochondria, respectively, 30 min after Ca^{2+} addition (Fig. 2a and b). Proteolysis/autolysis of calpain-5 was detected in the cytosol at 1 mM Ca^{2+} (Fig. 2c) but was readily observed for mitochondrial calpain-5 at concentrations greater than 5 μM Ca^{2+} (Fig. 2d).

3.2. Proteolysis/autolysis of mitochondrial calpain-5 in response to ER stress in HeLa cells

Calpain-5 was localized in the mitochondria of HeLa cells (Fig. 3a). To eliminate the possibility of subcellular contamination in mitochondrial fraction obtained from HeLa cells, we performed western blot analyses using the following organelle markers: GAPDH for cytosol, AK2 for mitochondria, calnexin for endoplasmic reticulum, and lamin A/C for nucleus. The results showed that highly purified mitochondrial fraction was obtained (Fig. 3b). To examine the effects of ER stress on calpain-5 proteolysis/autolysis in living cells, we treated HeLa cells with thapsigargin to induce mitochondrial Ca^{2+} uptake under ER stress. We separated the mitochondrial and cytosolic fractions from thapsigargin-

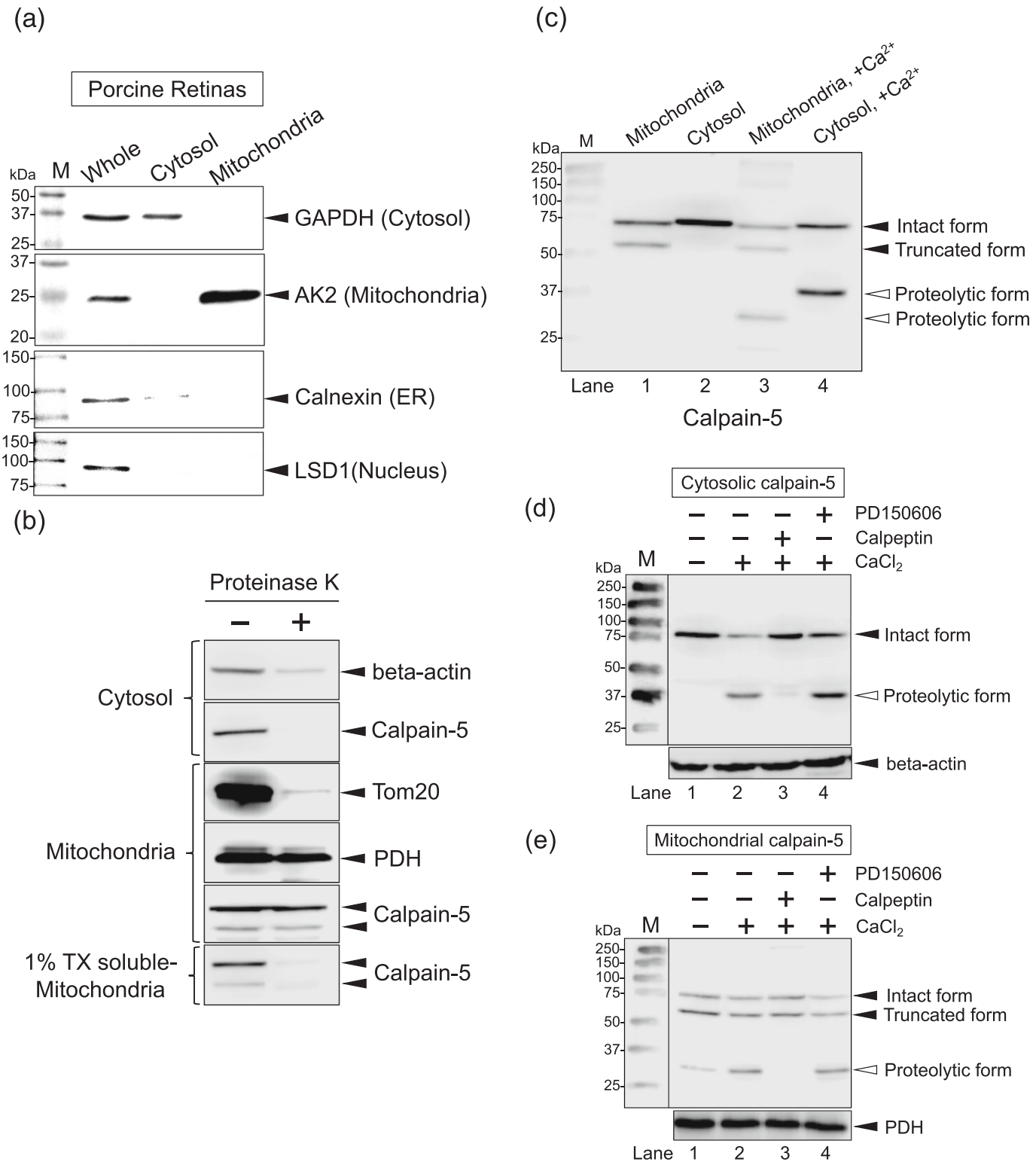

Fig. 1. Mitochondrial localization and proteolysis/autolysis of calpain-5 in porcine retinas. (a) The purity of the mitochondrial fraction was determined using the appropriate antibodies for the marker proteins [GAPDH, cytosol; AK2, mitochondria; calnexin, ER; LSD1, nucleus]. Highly purified mitochondrial fraction was obtained. (b–e) Antibodies against calpain-5 and specific marker proteins, including beta-actin, Tom20, and PDH, were used; 30 μg of proteins were applied to each lane. Representative results of three independent experiments are shown. (b) Western blot analysis of calpain-5 in proteinase K-treated mitochondria. Isolated mitochondria were treated with 100 μg/mL proteinase K for 30 min at 4 °C. Cytosolic fraction and soluble mitochondria in 1% Triton X-100 were used as a positive control to confirm that proteinase K was activated. Calpain-5 was detected in proteinase K-treated mitochondria. (c) Western blot analysis of calpain-5 in Ca^{2+}-incubated mitochondria. Intact forms of cytosolic and mitochondrial calpain-5 were ~75 kDa and ~70 kDa, respectively (lanes 1 and 2). Cytosolic and mitochondrial calpain-5 produced proteolytic/autolytic fragments of ~37 kDa and ~30 kDa, respectively, in the presence of Ca^{2+} (lanes 3 and 4). (d and e) The effects of calpain inhibitors on proteolysis/autolysis of cytosolic and mitochondrial calpain-5 in the presence of 5 μM PD150606, 10 μM calpeptin, or 1 mM Ca^{2+} for 120 min at 37 °C. Calpeptin inhibited proteolysis/autolysis of calpain-5 in each fraction but PD150606 did not.

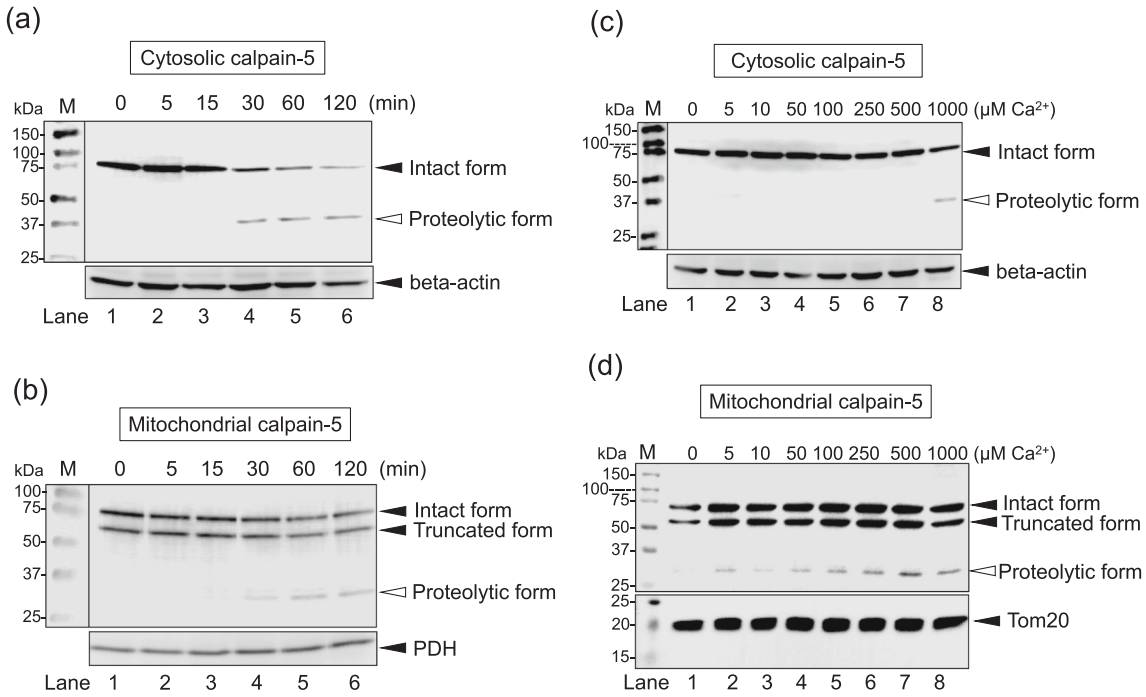

Fig. 2. Time- and Ca^{2+}-dependency of calpain-5 proteolysis/autolysis in porcine retinas. (a) Proteolysis/autolysis of cytosolic calpain-5 in the presence of 1 mM Ca^{2+} at 37 °C. (b) Proteolysis/autolysis of mitochondrial calpain-5 in the presence of 1 mM Ca^{2+} at 37 °C. (c) Proteolysis/autolysis of cytosolic calpain-5 in different Ca^{2+} concentrations for 120 min at 37 °C. (d) Proteolysis/autolysis of mitochondrial calpain-5 in different Ca^{2+} concentrations for 120 min at 37 °C. Beta-actin (cytosol), PDH and Tom20 (mitochondria) were used as loading controls; 30 μg of proteins were applied to each lane. Representative results of three independent experiments are shown.

treated HeLa cells and determined the proteolytic/autolytic fragments of calpain-5 *via* a western blot analysis for each fraction. The results showed that proteolytic/autolytic fragments of ~27 kDa for mitochondrial calpain-5 were detected at 12 h after the treatment with thapsigargin (Fig. 3d). However, cytosolic calpain-5 was not activated in thapsigargin-treated cells (Fig. 3c). Further, we examined the presence of cleaved ATF6, an ER stress marker. The levels of full length ATF6 decreased, while those of cleaved ATF6 increased following the treatment with thapsigargin (Fig. 3e). Therefore, our results indicated that mitochondrial calpain-5 was proteolyzed/autolyzed in response to ER stress.

3.3. Cell viability and ATP concentration in CAPN5 knockdown HeLa cells

CAPN1, *CAPN2*, *GAPDH*, and *CAPN5* knockdown in HeLa cells was performed by the transfection of specific siRNA, and the transfected cells exhibited decreased levels of calpain-1, calpain-2, calpain-5, and GAPDH proteins, respectively (Fig. 4a–d). Cell viability was significantly decreased in *CAPN5* and *GAPDH* knockdown cells, but not in *CAPN1* or *CAPN2* knockdown cells (Fig. 4e). ATP concentration was significantly decreased in *GAPDH* knockdown cells, but not in any of the other knockdowns (Fig. 4f). Therefore, our results indicated that calpain-5 modulates cell survival.

3.4. Characterization of cytosolic and mitochondrial calpain-5 in the mouse liver

To confirm the purity of the cytosolic and mitochondrial fractions obtained from mouse livers, we performed western blot analyses using the following organelle markers: GAPDH for cytosol, AK2 for mitochondria, calnexin for endoplasmic reticulum, and LSD1 for nucleus. Highly purified mitochondrial fraction was obtained (Fig. 5a). We determined the characteristics of mitochondrial calpain-5 in the mouse liver. Calpain-5 was detected in the mitochondrial fraction following Proteinase K treatment to remove proteins from the outer surface of the mitochondrial outer membranes (Fig. 5b). The molecular weights of the intact and truncated forms of mitochondrial calpain-5 were ~70 kDa and ~55 kDa, respectively (Fig. 5c). Next, we performed proteolysis/autolysis assays to examine the Ca^{2+} sensitivity of cytosolic and mitochondrial calpain-5 in the mouse liver. Although cytosolic calpain-5 was not proteolyzed/autolyzed in the presence of Ca^{2+} (Fig. 5d), the ~45 kDa proteolytic/autolytic fragments of mitochondrial calpain-5 were detected after Ca^{2+} addition (Fig. 5e). The proteolysis/autolysis of mitochondrial calpain-5 was inhibited by the pan-calpain inhibitor, calpeptin (Fig. 5e). Moreover, the ~70 kDa intact forms were decreased, and the ~45 kDa proteolytic/autolytic forms were increased in a time-dependent manner (Fig. 5f).

3.5. Proteolysis/autolysis of mitochondrial calpain-5 in ER stress-induced mouse liver

To investigate the proteolysis/autolysis of cytosolic and mitochondrial calpain-5 in animals, we examined the cleavage of calpain-5 in ER stress-induced mouse livers (Fig. 6). Tunicamycin was injected intraperitoneally into C57BL/6J mice to induce ER stress, as has been previously reported [20,21], and hepatic steatosis was observed following tunicamycin injection (Fig. 6a). We also found that the ER stress markers, *i.e.*, cleaved ATF6 and CHOP, were detected in the tunicamycin-injected mouse liver (Fig. 6b). Proteolysis/autolysis of calpain-5 was not detected in the cytosolic fraction of tunicamycin injected mouse livers, and the overall level of protein expression in these livers were unchanged (Fig. 6c). Interestingly, the levels of truncated calpain-5 in the mitochondria of tunicamycin treated mice were decreased and cleaved fragments of ~40 kDa were detected (Fig. 6d). Western blot analyses showed the increased expression of Bip and mitochondrial cytochrome *c*, whereas the expression of cytosolic cytochrome *c* was unchanged (Fig. 6e–h). These results suggest that the

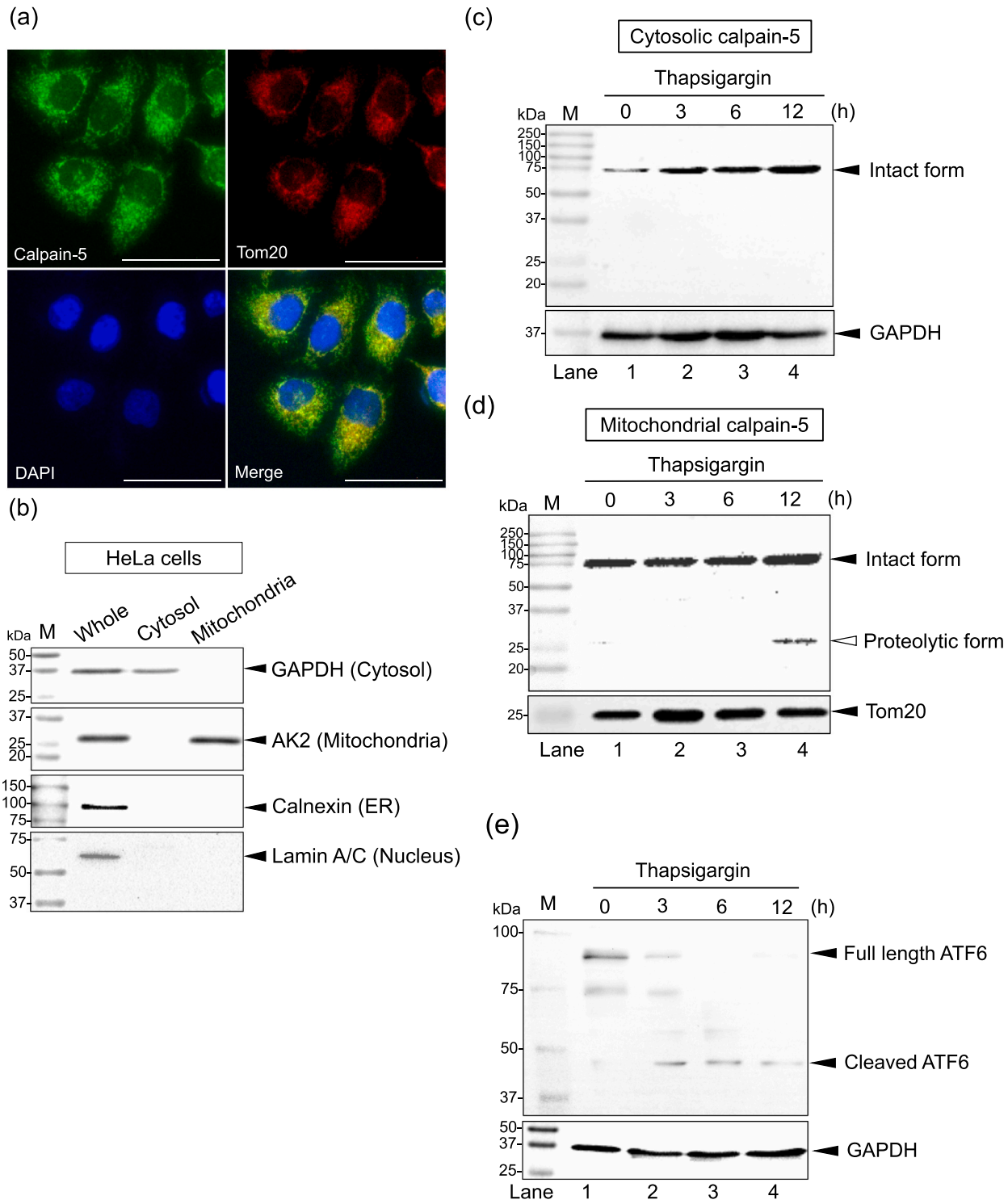

Fig. 3. Immunocytochemistry and western blot analyses of calpain-5 in HeLa cells treated with thapsigargin. (a) Immunocytochemistry of calpain-5, which was mainly localized in the mitochondria. Green, calpain-5; Red, Tom20 (mitochondrial marker); Blue, DAPI. Scale bars: 50 μm. (b) The purity of the mitochondrial fraction was determined using the appropriate antibodies for the marker proteins [GAPDH, cytosol; AK2, mitochondria; calnexin, ER; lamin A/C, nucleus] (20 μg/lane). Highly purified mitochondrial fraction was obtained. (c) Time-dependency of cytosolic calpain-5 proteolysis/autolysis in thapsigargin-treated HeLa cells. GAPDH was used as a loading control for the cytosolic fraction. Thirty μg of proteins were used in each lane. (d) Time-dependency of mitochondrial calpain-5 proteolysis/autolysis in thapsigargin-treated HeLa cells. Tom20 was used as a loading control for the mitochondrial fraction. Thirty μg of proteins were used for each lane. (e) Western blot analyses of an ER stress marker, ATF6, in thapsigargin-treated HeLa cells. GAPDH was detected as a loading control. Thirty μg of proteins were used in each lane. Representative results of three independent experiments are shown.

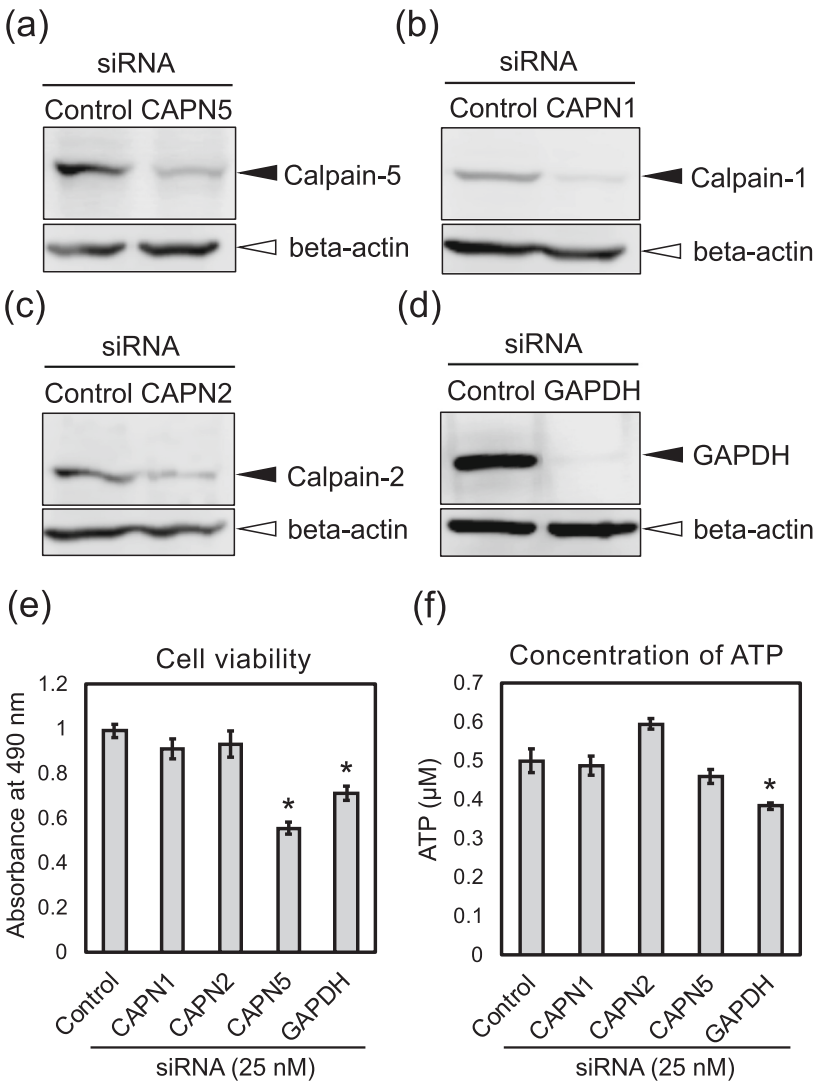

Fig. 4. Cell viability and ATP concentrations in calpain-5-knockdown HeLa cells. (a–d) Western blot analyses following knockdown of calpain-1, 2, 5, or GAPDH with siRNA; 30 μg of proteins were used for each lane. Anti-beta-actin antibody was used as a loading control. (e) Viability of HeLa cells 96 h after transfection of each siRNA. Data are shown as mean ± standard error [n = 6]. The Mann-Whitney *U* test was used to determine the significance of the difference between samples. *P* values were adjusted for multiple comparisons using the Bonferroni correction. * indicates $P < 0.05$ *vs.* control siRNA ($P = 0.008$, CAPN5 *vs* Control; $P = 0.008$, GAPDH vs Control). (f) The intracellular concentration of ATP in HeLa cells 96 h after transfection of each siRNA. Data are shown as mean ± standard error [n = 6]. The Mann-Whitney U test was used to determine the significance of the difference between samples. *P* values were adjusted for multiple comparisons using the Bonferroni correction. * = $P < 0.05$ *vs.* control siRNA ($P = 0.036$, GAPDH *vs* Control). Representative results of three independent experiments are shown.

activation of mitochondrial calpain-5 occurs in the early phases of ER stress in mouse livers. Next, we measured mitochondrial activity when mitochondrial calpain-5 was proteolyzed/autolyzed during ER stress in the mouse liver. The results showed that the integrity of the mitochondrial outer membrane was significantly decreased after treatment with tunicamycin in mouse livers (Fig. 6i), indicating that the activation of mitochondrial calpain-5 may affect mitochondrial activity.

4. Discussion

As per our knowledge, the present study is the first to characterize the proteolytic/autolytic properties and activation profiles of mitochondrial calpain-5 using porcine retinas, HeLa cells, and C57BL/6J mice. Our results demonstrated that mitochondrial calpain-5 was activated at low concentrations of Ca^{2+} during the early phases of ER stress. This finding suggests that mitochondrial calpain-5 may be involved in the response to ER stress.

The 15 well-conserved calpain isoforms exhibit unique activation characteristics. For example, calpain-3 rapidly undergoes autolytic cleavage and is activated by Ca^{2+} and Na^{+} [22]. In humans and mice, calpain-6 is inactive due to the absence of a cysteine in the active site [23]. Typically, the activation of calpains requires the binding of Ca^{2+} to the penta-EF (PEF) domain, as in calpain-1 and calpain-2. Calpain-5 contains a C2-like domain at the C-terminus, but not a PEF domain, suggesting the existence of an atypical activation mechanism. In this study, we showed that mitochondrial calpain-5 is activated at low Ca^{2+} concentrations (Fig. 2), indicating that cytosolic and mitochondrial calpain-5 have different sensitivities to Ca^{2+}. We propose that mitochondrial calpain-5 is an alternative splicing variant of cytosolic calpain-5 and that the three-dimensional conformation of the two structures is likely different. Despite this structural difference, the proteolysis/autolysis of both cytosolic and mitochondrial calpain-5 was inhibited by calpeptin. This similarity suggests that the active site of calpain-5 is conserved between mitochondrial and cytosolic calpain-5. Our results showed that PD150606 did not inhibit the proteolysis/autolysis of calpain-5. PD150606 is known to be a calpain-specific inhibitor due to its ability to target the PEF-hand domain, which is absent in calpain-5. However, Low et al. reported that the inhibitor must be acting at a site on the protease core domain of calpain-1 [24]. The group also showed that PD150606 did not bind to the PEF-hand of calpain-2 [24]. Considering these and the results of our present study, we suggest that PD150606 could not bind to the protease core domain of calpain-5, resulting in no inhibition of calpain-5 proteolysis/autolysis.

Further, we found that the molecular weight of the intact and proteolyzed/autolyzed mitochondrial calpain-5 was slightly lower than that of its cytosolic counterpart. We have previously reported that the molecular weight of calpain-5 in the mitochondrial fraction of porcine retinas differs from that of the cytosolic fraction [14]. Schaefer et al. have reported that most missense variants of calpain-5 exist in the N-terminal domain I, and splice-site variants were found in the protease

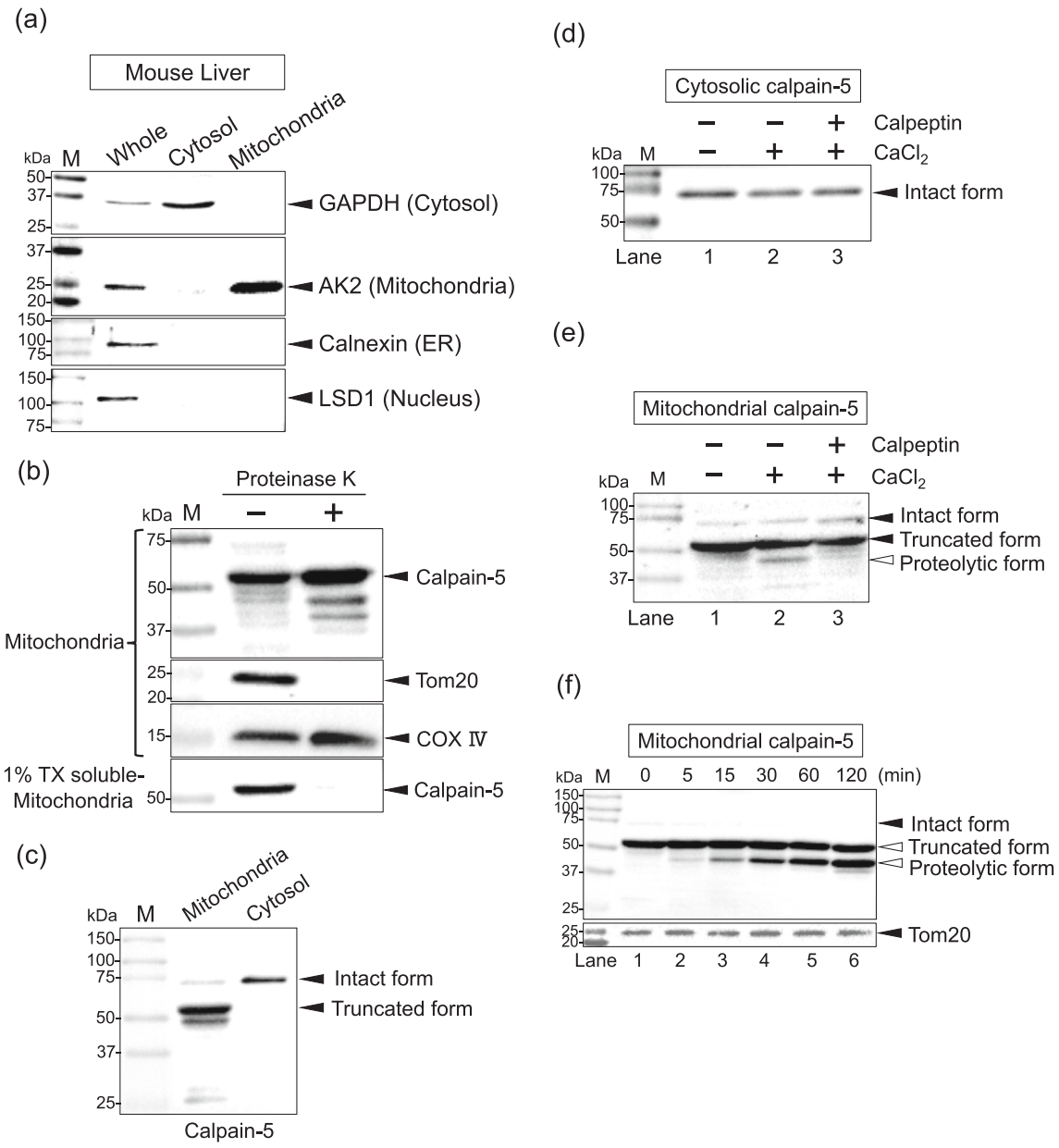

Fig. 5. Mitochondrial localization and proteolysis/autolysis of calpain-5 in mouse livers. (a) The purity of the mitochondrial fraction was determined using the appropriate antibodies for the marker proteins [GAPDH, cytosol; AK2, mitochondria; calnexin, ER; LSD1, nucleus]. Highly purified mitochondrial fraction was obtained. (b–f) Antibodies against calpain-5, Tom20 (a marker protein of the mitochondrial outer membrane), and COXIV (a marker protein of the mitochondrial inner membrane) were used; 40 μg of proteins were used for each lane. (b) Western blot analysis of calpain-5 in proteinase K-treated mitochondria. Soluble mitochondria in 1% Triton X-100 were used as a positive control to confirm that proteinase K was activated. Calpain-5 was detected in proteinase K-treated mitochondria. (c) Western blot analysis of cytosolic and mitochondrial calpain-5. Intact forms of mitochondrial and cytosolic calpain-5 were ~ 70 kDa. The truncated form of mitochondrial calpain-5 was ~55 kDa. (d and e) The effects of a calpain inhibitor on the proteolysis/autolysis of cytosolic and mitochondrial calpain-5 in the presence of 10 μM calpeptin or 1 mM Ca^{2+} for 120 min at 37 °C. Calpeptin inhibited proteolysis/autolysis of mitochondrial calpain-5. (f) Time-dependency of mitochondrial calpain-5 proteolysis/autolysis in the presence of 1 mM Ca^{2+}. The proteolytic/autolytic form of mitochondrial calpain-5 was ~45 kDa. Representative results of three independent experiments are shown.

core domain IIa outside the proteolytic core, demonstrating the potential heterogeneity of calpain-5 [25]. Together with the results of this study, it is reasonable to conclude that mitochondrial calpain-5 is a splicing variant of cytosolic calpain-5, resulting in its translocation to the mitochondria, the occurrence of conformational changes, and resultant different enzymatic properties. Further, the purification of mitochondrial calpain-5 should be performed to analyze its crystal structure in the near future.

Mitochondrial calpain-5 was activated in HeLa cells treated with thapsigargin that induces ER stress. ER stress in these cells was confirmed by the detection of cleaved ATF6, an ER stress marker (Fig. 3e). Furthermore, RNA interference against *CAPN1* and *CAPN2* did not influence cell viability, whereas the knockdown of *CAPN5* caused a decrease in cell viability (Fig. 4e). These findings demonstrate the essential role played by calpain-5 in various physiological processes during ER stress. In tunicamycin-treated mice, intact and truncated mitochondrial calpain-5 was dramatically decreased, and, correspondingly, its proteolytic/autolytic fragment was increased, whereas cytosolic calpain-5 remained unchanged (Fig. 6c and d). These results suggest that mitochondrial calpain-5 was sensitive to ER stress and could

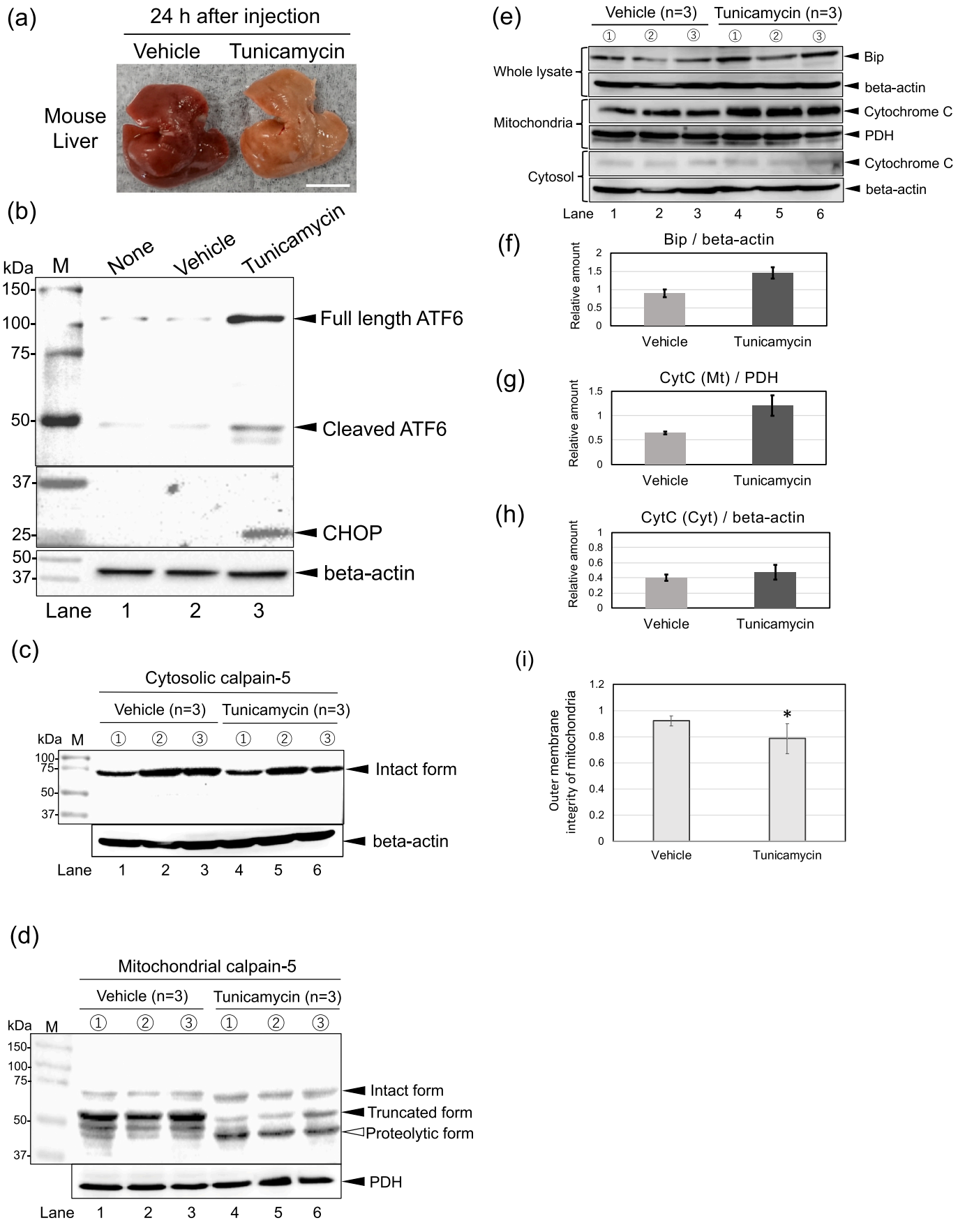

(caption on next page)

Fig. 6. Proteolysis/autolysis of mitochondrial calpain-5 in tunicamycin-treated C57BL/6J mouse liver. (a) Morphology of tunicamycin or vehicle-injected mouse liver. Scale bars: 1 cm. (b) Western blot analyses of the ER stress markers, full length and cleaved ATF6 and CHOP, in tunicamycin-treated mouse liver. Anti-beta-actin antibody was used as a loading control. (c) Western blot analyses of cytosolic calpain-5 in tunicamycin-treated mouse liver. The sample consisted of cytosolic fractions obtained from mouse livers (n = 3 mice per group); 40 μg of proteins were used for each lane. Anti-beta-actin antibody was used as a loading control. (d) Western blot analyses of mitochondrial calpain-5 in tunicamycin-treated mouse liver. The sample consisted of mitochondrial fractions obtained from mouse livers (n = 3 mice per group); 40 μg of proteins were used for each lane. Anti-PDH antibody was used as a loading control. Representative results of three independent experiments are shown. (e) Western blot analyses of Bip, beta-actin, cytochrome *c*, and PDH in tunicamycin-treated mouse liver. Each sample was a whole cell lysate, mitochondrial fraction, and cytosolic fraction of tunicamycin, or vehicle-treated mouse livers (n = 3 mice per group); 40 μg of proteins were used for each lane. (f) Relative amounts of Bip and beta-actin. (g) Relative amounts of mitochondrial cytochrome C [CytC (Mt)] and PDH. (h) Relative amounts of cytosolic cytochrome C [CytC (Cyt)] and beta-actin. (i) Outer membrane integrity of mitochondria in tunicamycin-treated mouse liver. The Mann-Whitney U test was used to determine the significance of differences between samples. * indicates $P < 0.05$ *vs.* vehicle ($P = 0.026$).

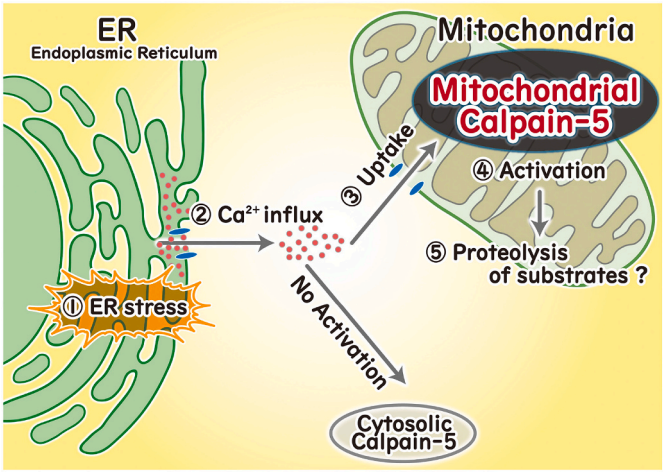

Fig. 7. Proposed model of mitochondrial calpain-5 activation during ER stress. Ca^{2+} is released through ryanodine receptors and inositol 1,4,5-triphosphate receptors under ER stress. Ca^{2+} influx from the ER induces an increase of cytosolic Ca^{2+}. Uptake of cytosolic Ca^{2+} by mitochondria results in the activation of mitochondrial calpain-5. Active mitochondrial calpain-5 would proteolyze the substrates in the mitochondria during the early phases of ER stress.

be activated more easily during ER stress than cytosolic calpain-5. Results from recent studies support our results indicating that ER stress induced calpain activation [26,27]. Xie et al. reported that Ca^{2+}-dependent calpain-2 activity promoted the ER stress-related cell death of rat hepatocytes by activating caspase-12 in the ER [26]. Mohsin et al. reported that ER stress-mediated activation of mitochondrial calpain-1 and calpain-2 contributed to complex I damage by cleaving component subunits, including NDUFS7, in cardiac mitochondria [27]. To the best of our knowledge, this is the first study to report that mitochondrial calpain-5 is activated during ER stress.

Based on our results, we have proposed a model for the activation of mitochondrial calpain-5 under ER stress (Fig. 7). The ER stores about 100–800 μM Ca^{2+}, which is released through ryanodine receptors and inositol 1,4,5-triphosphate receptors during ER stress [28]. Ca^{2+} efflux from the ER increases cytosolic Ca^{2+} levels and, in turn, the mitochondrial uptake of Ca^{2+} from the cytosol [29]. Our results suggest that mitochondrial calpain-5 may be activated in response to the mitochondrial uptake of Ca^{2+} released by the ER during stress, but cytosolic calpain-5 is not, demonstrating a mechanism by which mitochondrial calpain-5 may be involved in the cellular response to ER stress. During the early phases of ER stress, mitochondrial metabolism is increased to supply sufficient ATP for chaperones involved in relieving ER stress [30,31]. Although it is known that isocitrate, alpha-ketoglutarate, and pyruvate dehydrogenases are activated to produce ATP in response to the increase in mitochondrial Ca^{2+} [32], other factors that contribute to increased ATP production upon Ca^{2+} stimulation are poorly understood. The present study showed that tunicamycin treatment led to an increase in cytochrome *c* content in the mitochondria, suggesting that activated calpain-5 may lead to the translocation of transcription factors into the nucleus by mitochondrial-nuclear communication and activate the transcription of cytochrome *c*, resulting in an increase in cytochrome *c* content within the mitochondria. Considering this potential mechanism, we suggest that the activation of mitochondrial calpain-5 may facilitate ATP production during the early phases of ER stress. Future studies will explore the potential value of calpain-5 as a therapeutic approach for the treatment of ER stress-associated diseases, including neurodegenerative diseases, metabolic syndromes, diabetes, and cancer.

We demonstrated that the molecular weights of the proteolytic/autolytic fragments of mitochondrial calpain-5 varied depending on the species including pigs, humans, and mice. In porcine retinas, the molecular weight of the proteolytic/autolytic fragments of mitochondrial calpain-5 was ~30 kDa (Figs. 1 and 2). In human HeLa cells, the molecular weight of the proteolytic/autolytic fragments of mitochondrial calpain-5 was ~27 kDa (Fig. 3). In mouse livers, the molecular weight of the proteolytic/autolytic fragments of mitochondrial calpain-5 was ~40 kDa (Figs. 5 and 6). Further, we performed a homology search of calpain-5 among the species to compare the amino acid residues by the ESPript3 program (http://esprit.ibcp.fr/ESPript/index.php) [33]. The results showed that the sequence is highly conserved among humans, pigs, and mice (Supplementary Fig. 1). We suggest that the differences in molecular weights of the proteolytic/autolytic fragments contribute to three-dimensional structures or regulatory proteins associated with mitochondrial calpain-5. In the future, the differences between the species should be clarified.

In mouse liver mitochondria, we found that the truncated calpain-5 was protected from proteolysis/autolysis *in vitro* Ca^{2+}-incubation (Fig. 5f). However, in ER stress-induced mouse livers, the truncated form decreased and the proteolytic/autolytic form increased *in vivo* (Fig. 6d). Calpain-1 and -2 require high concentration of Ca^{2+} for activation *in vitro*, which is not achievable *in vivo* [1]. Therefore, there are differences between the calpain activation *in vivo* and *in vitro*. One possibility for these differences is the endogenous modulators such as phospholipids and calpastatin. Therefore, elucidating the activation mechanism of calpain-5 is required in future studies.

The present study is limited by our inability to directly measure calpain-5 activity, and therefore, we relied on the measurement of proteolysis/autolysis as an indirect indication of activation. Substrates for calpain-5 remains unknown, which necessarily limits the direct evaluation of enzyme activity. Hence, the identification of the substrate of calpain-5 warrants further study. In addition, we could not determine whether the Ca^{2+}-mediated processing of calpain-5 was due to autolysis or proteolysis by other proteases, including other calpains. Therefore, it is necessary to purify calpain-5 and determine its autolysis/proteolysis in future studies. Furthermore, while the apparent difference in molecular weight indicates some variation between mitochondrial and cytosolic calpain-5, mitochondrial calpain-5 remains to be purified to elucidate the differences in the secondary and tertiary structures of mitochondrial and cytosolic calpain-5.

In summary, we have demonstrated that mitochondrial calpain-5 was activated at low Ca^{2+} concentrations *in vitro* and during the early phases of ER stress *in vivo*. Additionally, we have provided new insights into the role of mitochondrial calpain-5 in cellular responses to ER stress.

Supplementary data to this article can be found online at https://doi.org/10.1016/j.bbamcr.2021.118989.

Fuding

The work was supported in part by JSPS KAKENHI [grant number JP16K20298, Grant-in-Aid for Young Scientists (B) for Taku Ozaki] the Uehara Memorial Foundation for Taku Ozaki.

Role of the sponsor

The funding organizations had no role in the design, conducting the study, data collection, management, analysis, interpretation, preparation, or review. The funding organization had no role in the approval of the manuscript or the decision to submit the manuscript for publication.

Data statement

The data from this study are available from the corresponding author, Taku Ozaki, upon reasonable request.

CRediT authorship contribution statement

Yusaku Chukai: Formal analysis, Validation, Investigation, Visualization, Writing – original draft. **Takeshi Iwamoto:** Formal analysis, Investigation, Data curation, Writing – original draft. **Ken Itoh:** Methodology, Validation, Writing – review & editing. **Hiroshi Tomita:** Resources. **Taku Ozaki:** Conceptualization, Methodology, Validation, Investigation, Writing – original draft, Writing – review & editing, Visualization, Supervision, Project administration, Funding acquisition.

Declaration of competing interest

There are no conflicts of interest to declare.

Acknowledgments

We would like to thank Prof. Tetsuro Yamashita for carefully proofreading the manuscript and Ms. Satomi Fujisaki for assistance creating illustrations.

References

[1] D.E. Goll, V.F. Thompson, H. Li, W. Wei, J. Cong, The calpain system, Physiol. Rev. 83 (2003) 731–801, https://doi.org/10.1152/physrev.00029.2002.
[2] Y. Ono, H. Sorimachi, Calpains - an elaborate proteolytic system, Biochim. Biophys. Acta Protein Proteomics 1824 (2012) 224–236, https://doi.org/10.1016/j.bbapap.2011.08.005.
[3] M. Hosseini, H. Najmabadi, K. Kahrizi, Calpains: diverse functions but enigmatic, Arch. Iran. Med. 21 (2018) 170–179.
[4] M.A. Smith, R.G. Schnellmann, Calpains, mitochondria, and apoptosis, Cardiovasc. Res. 96 (2012) 32–37, https://doi.org/10.1093/cvr/cvs163.
[5] V.B. Mahajan, J.M. Skeie, A.G. Bassuk, J.H. Fingert, T.A. Braun, H.T. Daggett, J. C. Folk, V.C. Sheffield, E.M. Stone, Calpain-5 mutations cause autoimmune uveitis, retinal neovascularization, and photoreceptor degeneration, PLoS Genet. 8 (2012) 2–10, https://doi.org/10.1371/journal.pgen.1003001.
[6] K.J. Wert, S.F. Koch, G. Velez, C.W. Hsu, M.A. Mahajan, A.G. Bassuk, S.H. Tsang, V. B. Mahajan, CAPN5 genetic inactivation phenotype supports therapeutic inhibition trials, Hum. Mutat. 40 (2019) 2377–2392, https://doi.org/10.1002/humu.23894.
[7] G. Velez, Y.J. Sun, S. Khan, J. Yang, J. Herrmann, T. Chemudupati, R.E. MacLaren, L. Gakhar, S. Wakatsuki, A.G. Bassuk, V.B. Mahajan, Structural insights into the unique activation mechanisms of a non-classical calpain and its disease-causing variants, Cell Rep. 30 (2020) 881–892, https://doi.org/10.1016/j.celrep.2019.12.077.
[8] T. Franz, L. Winckler, T. Boehm, T.N. Dear, Capn5 is expressed in a subset of T cells and is dispensable for development, Mol. Cell. Biol. 24 (2004) 1649–1654, https://doi.org/10.1128/mcb.24.4.1649-1654.2004.
[9] T. Ozaki, H. Tomita, M. Tamai, S.I. Ishiguro, Characteristics of mitochondrial calpains, J. Biochem. 142 (2007) 365–376, https://doi.org/10.1093/jb/mvm143.
[10] T. Ozaki, T. Yamashita, S.I. Ishiguro, ERp57-associated mitochondrial μ-calpain truncates apoptosis-inducing factor, Biochim. Biophys. Acta 1783 (2008) 1955–1963, https://doi.org/10.1016/j.bbamcr.2008.05.011.
[11] T. Ozaki, T. Yamashita, S.I. Ishiguro, Mitochondrial m-calpain plays a role in the release of truncated apoptosis-inducing factor from the mitochondria, Biochim. Biophys. Acta 1793 (2009) 1848–1859, https://doi.org/10.1016/j.bbamcr.2009.10.002.
[12] A. Waghray, D.S. Wang, D. McKinsey, R.L. Hayes, K.K.W. Wang, Molecular cloning and characterization of rat and human calpain-5, Biochem. Biophys. Res. Commun. 324 (2004) 46–51, https://doi.org/10.1016/j.bbrc.2004.09.012.
[13] R. Singh, M.K. Brewer, C.B. Mashburn, D. Lou, V. Bondada, B. Graham, J. W. Geddes, Calpain 5 is highly expressed in the central nervous system (CNS), carries dual nuclear localization signals, and is associated with nuclear promyelocytic leukemia protein bodies, J. Biol. Chem. 289 (2014) 19383–19394, https://doi.org/10.1074/jbc.M114.575159.
[14] T. Iwamoto, E. Ishiyama, K. Ishida, T. Yamashita, H. Tomita, Presence of calpain-5 in mitochondria, Biochem. Biophys. Res. Commun. 504 (2018) 454–459, https://doi.org/10.1016/j.bbrc.2018.08.144.
[15] S. Utsumi, K. Sakamoto, T. Yamashita, H. Tomita, E. Sugano, K. Ishida, E. Ishiyama, T. Ozaki, Presence of ES1 homolog in the mitochondrial intermembrane space of porcine retinal cells, Biochem. Biophys. Res. Commun. 524 (2020) 542–548, https://doi.org/10.1016/j.bbrc.2020.01.127.
[16] A. Baki, P. Tompa, A. Alexa, O. Molnár, P. Friedrich, Autolysis parallels activation of mu-calpain, Biochem. J. 318 (1996) 897–901, https://doi.org/10.1042/bj3180897.
[17] J.S. Chou, F. Impens, K. Gevaert, P.L. Davies, m-Calpain activation in vitro does not require autolysis or subunit dissociation, Biochim. Biophys. Acta Protein Proteomics 1814 (2011) 864–872, https://doi.org/10.1016/j.bbapap.2011.04.007.
[18] R.L. Campbell, P.L. Davies, Structure-function relationships in calpains, Biochem. J. 447 (2012) 335–351, https://doi.org/10.1042/BJ20120921.
[19] Y. Tomita, T. Yamashita, H. Sato, H. Taira, Kinetics of interactions of sendai virus envelope glycoproteins, F and HN, with endoplasmic reticulum-resident molecular chaperones, BiP, calnexin, and calreticulin, J. Biochem. 126 (1999) 1090–1100, https://doi.org/10.1093/oxfordjournals.jbchem.a022554.
[20] B. Feng, X. Huang, D. Jiang, L. Hua, Y. Zhuo, D. Wu, Endoplasmic reticulum stress inducer tunicamycin alters hepatic energy homeostasis in mice, Int. J. Mol. Sci. 18 (2017) 1710, https://doi.org/10.3390/ijms18081710.
[21] A. Abdullahi, M. Stanojcic, A. Parousis, D. Patsouris, M.G. Jeschke, Modeling acute ER stress in vivo and in vitro, Shock 47 (2017) 506–513, https://doi.org/10.1097/SHK.0000000000000759.
[22] Y. Ono, K. Ojima, F. Shinkai-ouchi, S. Hata, H. Sorimachi, Biochimie 122 (2016) 169–187, https://doi.org/10.1016/j.biochi.2015.09.010.
[23] K. Tonami, S. Hata, K. Ojima, Y. Ono, Y. Kurihara, T. Amano, T. Sato, Y. Kawamura, H. Kurihara, H. Sorimachi, Calpain-6 deficiency promotes skeletal muscle development and regeneration, PLoS Genet. 9 (2013) 1–11, https://doi.org/10.1371/journal.pgen.1003668.
[24] K.E. Low, S.K. Partha, P.L. Davies, R.L. Campbell, Allosteric inhibitors of calpains: reevaluating inhibition by PD150606 and LSEAL, Biochim. Biophys. Acta 1840 (2014) 3367–3373, https://doi.org/10.1016/j.bbagen.2014.08.014.
[25] K.A. Schaefer, M.A. Toral, G. Velez, A.J. Cox, S.A. Baker, N.C. Borcherding, D. F. Colgan, V. Bondada, C.B. Mashburn, C.G. Yu, J.W. Geddes, S.H. Tsang, A. G. Bassuk, V.B. Mahajan, Calpain-5 expression in the retina localizes to photoreceptor synapses, Invest. Ophthalmol. Vis. Sci. 57 (2016) 2509–2521, https://doi.org/10.1167/iovs.15-18680.
[26] R.J. Xie, X.X. Hu, L. Zheng, S. Cai, Y.S. Chen, Y. Yang, T. Yang, B. Han, Q. Yang, World J. Gastroenterol. 26 (2020) 1450–1462, https://doi.org/10.3748/wjg.v26.i13.1450.
[27] A.A. Mohshin, J. Thompson, Y. Hu, J. Hollander, E.J. Lesnefsky, Q. Chen, Endoplasmic reticulum stress-induced complex I defect: central role of calcium overload, Arch. Biochem. Biophys. 683 (2020) 108299, https://doi.org/10.1016/j.abb.2020.108299.
[28] A. Carreras-Sureda, P. Pihán, C. Hetz, Calcium signaling at the endoplasmic reticulum: fine-tuning stress responses, Cell Calcium 70 (2018) 24–31, https://doi.org/10.1016/j.ceca.2017.08.004.
[29] A. Rossi, P. Pizzo, R. Filadi, Calcium , mitochondria and cell metabolism: a functional triangle in bioenergetics, Biochim. Biophys. Acta, Mol. Cell Res. 1866 (2019) 1068–1078, https://doi.org/10.1016/j.bbamcr.2018.10.016.
[30] R. Bravo, J.M. Vicencio, V. Parra, R. Troncoso, J.P. Munoz, M. Bui, C. Quiroga, A. E. Rodriguez, H.E. Verdejo, J. Ferreira, M. Iglewski, M. Chiong, T. Simmen, A. Zorzano, J.A. Hill, B.A. Rothermel, G. Szabadkai, S. Lavandero, Increased ER-mitochondrial coupling promotes mitochondrial respiration and bioenergetics during early phases of ER stress, J. Cell Sci. 124 (2011) 2511, https://doi.org/10.1242/jcs.080762.
[31] A. Burkart, X. Shi, M. Chouinard, S. Corvera, Adenylate kinase 2 links mitochondrial energy metabolism to the induction of the unfolded protein response, J. Biol. Chem. 286 (2011) 4081–4089, https://doi.org/10.1074/jbc.M110.134106.
[32] R. Bravo, T. Gutierrez, F. Paredes, D. Gatica, A.E. Rodriguez, Z. Pedrozo, M. Chiong, V. Parra, A.F.G. Quest, B.A. Rothermel, S. Lavandero, Endoplasmic reticulum: ER stress regulates mitochondrial bioenergetics, Int. J. Biochem. Cell Biol. 44 (2012) 16–20, https://doi.org/10.1016/j.biocel.2011.10.012.
[33] X. Robert, P. Gouet, Deciphering key features in protein structures with the new ENDscript server, Nucleic Acids Res. 42 (2014), W320-4.